Lab on a Chip

PAPER

View Article Online
View Journal | View Issue

Check for updates

Cite this: *Lab Chip*, 2019, **19**, 1436

# 3D impedimetric sensors as a tool for monitoring bacterial response to antibiotics†

S. Brosel-Oliu, [a] O. Mergel,[b] N. Uria, [a] N. Abramova, [ac] P. van Rijn [b] and A. Bratov [*a]

The presence of antimicrobial contaminants like antibiotics in the environment is a major concern because they promote the emergence and the spread of multidrug resistant bacteria. Since the conventional systems for the determination of bacterial susceptibility to antibiotics rely on culturing methods that require long processing times, the implementation of novel strategies is highly required for fast and point-of-care applications. Here the development and characterization of a novel label-free biosensing platform based on a microbial biosensor approach to perform antibiotic detection bioassays in diluted solution is presented. The microbial biosensor is based on a three-dimensional interdigitated electrode array (3D-IDEA) impedimetric transducer with immobilized *E. coli* bacteria. In 3D-IDEA to increase the sensitivity to superficial impedance changes the electrode digits are separated by insulating barriers. A novel strategy is employed to selectively immobilize bacteria in the spaces over the electrode digits between the barriers, referred to here as trenches, in order to concentrate bacteria, improve the reproducibility of the *E. coli* immobilization and increase the sensitivity for monitoring bacterial response. For effective attachment of bacteria within the trenches an initial anchoring layer of a highly charged polycation, polyethyleneimine (PEI), was used. To facilitate immobilization of bacteria within the trenches and prevent their deposition on top of the barriers an important novelty is the use of poly(*N*-isopropylmethacrylamide) p(NIPMAM) microgels working as antifouling agents, deposited on top of the barriers by microcontact printing. The reported microbial biosensor approach allows the bacterial response to ampicillin, a bacteriolytic antibiotic, to be registered by means of impedance variations in a rapid and label-free operation that enables new possibilities in bioassays for toxicity testing.

Received 7th November 2018,
Accepted 19th February 2019

DOI: 10.1039/c8lc01220b

rsc.li/loc

Open Access Article. Published on 20 February 2019. Downloaded on 5/12/2025 9:43:43 PM.
This article is licensed under a Creative Commons Attribution 3.0 Unported Licence.

## 1. Introduction

Infectious diseases and emerging bacterial pathogens are still one of the main public health problems worldwide.[1] In the last century different antimicrobial reagents like antibiotics have been employed for the prevention and treatment of bacterial infections.[2] Antibiotics are antimicrobial drugs of natural or synthetic origin mainly used for the treatment and prevention of infectious diseases in humans and employed to promote growth of animals in the meat industry.[3] However, the extensive and abusive use of antibiotics in healthcare, medicinal veterinary and even in agriculture has led to the appearance of bacterial resistance genes, which are promoted because antibiotics also act on commensal bacteria, creating a reservoir of resistant organisms.[4,5] Food and water are important vectors for the spreading of these resistant organisms between humans and animals, resulting in increasing pressure for ensuring safety in human consumption.[6] Hence, different methods are required to perform bacterial detection assays and identify possible antibiotic resistances in common pathogens.

The standard methods to study the required dosage of antibiotics are mainly based on antimicrobial susceptibility tests (AST), which are accomplished using classical microbiological methods or automated systems.[7–9] These methods, are not sufficiently fast, requiring 1–2 days of processing time to get reliable information, and can hardly be used for rapid diagnostics in point-of-care portable systems.[10] More recently, polymerase chain reaction (PCR) has been employed for the detection of resistant genes. However, these methods are expensive and have not been adopted yet for resistance detection assays.[11] Hence, novel technologies to study the

[a] *BioMEMS Group, Institute of Microelectronics of Barcelona (IMB-CNM, CSIC), Esfera UAB-CEI, Campus Universitat Autònoma de Barcelona, 08193 Bellaterra, Spain. E-mail: andrei.bratov@imb-cnm.csic.es; Tel: +34 935947700*
[b] *Department of Biomedical Engineering-FB40A, University of Groningen University Medical Center Groningen, Deusinglaan 1, 9713 AV, Groningen, The Netherlands*
[c] *Lab. Artificial Sensors Syst., ITMO University, Kronverskiy pr. 49, 197101 St. Petersburg, Russia*

† Electronic supplementary information (ESI) available. See DOI: 10.1039/c8lc01220b



This journal is © The Royal Society of Chemistry 2019

Open Access Article. Published on 20 February 2019. Downloaded on 5/12/2025 9:43:43 PM.
This article is licensed under a Creative Commons Attribution 3.0 Unported Licence.

effectiveness of antimicrobial drugs like antibiotics are in high demand.

A promising option is to monitor the response of bacterial cells to different treatments that affect their metabolic activity, the cell viability or structural changes. In this sense microbial biosensors, consisting of a transducer with immobilized microbial cells, are promising tools as they use the cellular response for the detection of biologically active agents.[12] A few works for the detection of antibiotics using microbial-based biosensors have been reported: for example, a potentiometric microbial biosensor to detect the presence of β-lactams, which inhibits the microbial growth,[13] or an optical whole-cell biosensor using engineered *P. putida* to detect structurally diverse antibiotics.[14] Despite the fact that different kinds of transducers may be employed to perform detection assays, a limited number of works report the study of susceptibility of bacteria to antimicrobial compounds.[15]

Among the electrochemical transducers, impedance-based sensors are really advantageous considering their ability to perform label-free detection,[16] low cost production, ease of miniaturization and integration with other technologies like microfluidics.[17] In the case of electrochemical impedance spectroscopy (EIS) the measurements may be performed in Faradaic and non-Faradaic modes. In the first case a redox couple in the electrolyte solution is required to transfer a charge across an interface, while in non-Faradaic measurements no additional reagent is necessary, and impedance mainly depends on the electrode interfacial capacitance.[18–20]

To perform impedance measurements different electrode formats may be selected. It has been demonstrated that interdigitated electrode array (IDEA) transducers, consisting of a pair of comb-like metal electrodes deposited on an insulating substrate, are really advantageous in terms of rapid detection kinetics, increased signal-to-noise ratio and fast establishment of a steady-state signal.[21] In addition, as the measurements are performed in a non-Faradaic mode without applying additional DC bias, the applied signal and the current response are measured between the pair of electrodes of an IDEA, eliminating the need for a reference electrode. As both electrodes are commonly of the same material it is assumed that the electric potential difference between them is close to zero. The impedance of the IDEA sensor in a water solution measured between a pair of electrodes mainly depends on the solution conductivity and interfacial capacitance of the electrodes.[22] In low conducting solutions, surface conductivity in the spacing between electrode digits may prevail over the bulk solution conductivity and play a significant role in the overall impedance.[20,23]

Recently, to enhance the sensitivity of standard planar IDEA devices a new design based on a three-dimensional interdigitated electrode array (3D-IDEA) sensor, in which an insulating barrier is introduced between the adjacent electrodes, was proposed.[23] The separation of the electrode digits of an IDEA by $SiO_2$ insulating barriers allows the enhancement of the effect of surface conductivity on the impedance measurements. In this case the penetration of the electric field into the bulk solution is the same as for a planar/flat IDEA with an equivalent geometry, but the current path along the $SiO_2$ surface is much longer, which permits the enhancement of the sensitivity of the device to surface conductivity changes. The applications of 3D-IDEA biosensors for label-free detection of bacteria have been reported earlier.[24,25] In these cases the 3D-IDEA sensor surface was functionalized with different biorecognition molecules to selectively detect bacteria or bacterial toxins.

Accordingly, taking into account the high sensitivity of these 3D-IDEA sensors in comparison with conventional planar IDEA,[23] we assume that these devices with immobilized bacteria may also be employed for monitoring the bacterial response to different antimicrobial compounds. It is well-known that among different antibiotics, ampicillin (Amp), of the β-lactam group, inhibits bacteria cell wall synthesis and induces cellular stress, which culminates in cell lysis.[26,27] Thus, the bacterial membrane integrity is affected, inducing a release of cytoplasmatic compounds outside.

In this work a new biosensing platform is developed using disposable three-dimensional interdigitated electrode arrays (3D-IDEA) as impedimetric transducers and *E. coli* bacterial cells as the recognition element against ampicillin. One of the main challenges is the development of a reproducible method of bacteria immobilization on the transducer unit as the reproducibility of bacterial attachment is an important limitation in the performance of microbial-based biosensors. To achieve this, specifically synthesized poly(*N*-isopropylmethacrylamide) (p(NIPMAM)) microgels (μGel) have been used.

Microgels have found considerable interest due their ability to encapsulate, protect, and release bioactive components. Polymeric microgels are spherical particles (typically in the size range between 100 nm and 1000 μm) whose interior consists of a three-dimensional cross-linked polymeric network that entraps a considerable amount of solvent.[28] One of the remarkable features of microgel particles is that they structurally respond to external stimuli like temperature, pH or electric field applied with conformational changes.[29] The use of microgels is reported in many fields, including biosensing applications, providing a favorable environment for enzymes and other biomolecules to preserve their activity and functional structure,[30] and also in triggered drug delivery systems.[31] In addition, due to their facility for tuning their structure and physical and chemical properties, microgels are also employed as antifouling agents in biointerfaces[32–34] preventing cell adhesion.

In this study we present a novel strategy for the spatially selective immobilization of *E. coli* bacteria cells in the spaces between the barriers of a 3D-IDEA, here referred to as "trenches". In this case, one of the main objectives of the work is to prevent the adhesion of bacteria on top of barriers. To achieve this, poly(*N*-isopropylmethacrylamide) (p(NIPMAM)) microgels were used as antifouling agents to avoid the attachment of *E. coli* on top of barriers. A highly positively charged polycation, polyethyleneimine (PEI), typically used for the formation of thin multilayer coatings was

Open Access Article. Published on 20 February 2019. Downloaded on 5/12/2025 9:43:43 PM.
This article is licensed under a Creative Commons Attribution 3.0 Unported Licence.

employed as an initial anchoring layer, allowing the p(NIPMAM) microgel attachment mainly by electrostatic interactions. Finally, the changes produced in the medium in the presence of ampicillin and *E. coli* bacteria were monitored in a micro-incubation chamber with a small volume specifically designed to perform the impedimetric measurements in a simple and easy-to-use format (Fig. 1).

The present study shows a promising biosensing approach that can be employed for the determination of antimicrobial drugs and can also be an attractive method for the detection of other toxic contaminants that can affect the bacterial integrity.

## 2. Materials and methods

### 2.1. Reagents and materials

The polycation polyethyleneimine (PEI, branched, average Mw 25 000, water-free) was dissolved in deionized water at 1.5 mg $mL^{-1}$ in accord with previously published works.[35] *N*-Isopropylmethacrylamide (97%, NIPMAM), the cross-linker *N*,*N*′-methylenebis(acrylamide) (99%, BIS), the surfactant sodium dodecyl sulfate (SDS) and the initiator ammonium persulfate (98% APS) were purchased from Sigma-Aldrich. The dye methacryloxyethyl thiocarbamoyl Rhodamine B (MRB) was purchased from Polysciences, Inc. *N*-Isopropylmethacrylamide was recrystallized from hexane. The polydimethylsiloxane (PDMS) elastomer substrate was obtained by mixing 18 g of the prepolymer (Sylgard 184A) and cross-linker (Sylgard 184B, Dow Corning), vigorously stirred with a spatula at a 10 : 1 ratio. The viscous mixture was deposited on a 12 × 12 cm clean squared petri dish under vacuum to eliminate the bubbles and cured at 70 °C in an oven overnight. Ampicillin sodium salt was dissolved in water at 10 mg $mL^{-1}$ to obtain a stock solution that was diluted till the desired concentration.

All the solutions were prepared with deionized ultrapure water (18.2 MΩ cm, arium 611 DI water purification system; Sartorius AG, Göttingen, Germany) which was also used for the cleaning and rinsing processes. Except for *N*-isopropylmethacrylamide, all the chemicals were of analytical grade and were used as received without any further purification.

### 2.2. Fabrication of 3D-IDEA sensors

3D-IDEA sensors were fabricated using conventional microelectronic techniques. The interdigitated electrode array was formed on a silicon wafer covered with a 2.5 mm thick thermal silicon oxide layer. As an electrode material, a highly conductive tantalum silicide ($TaSi_2$) was deposited using magnetron sputtering. This layer was patterned using conventional lithography giving as a result interdigitated electrodes with 216 digits of 3 μm width and 3 μm gap between the adjacent electrodes. The aperture between the electrodes is 1.4 mm and the total length between the electrodes is 301 mm. The wafer was covered by a 4 μm thick

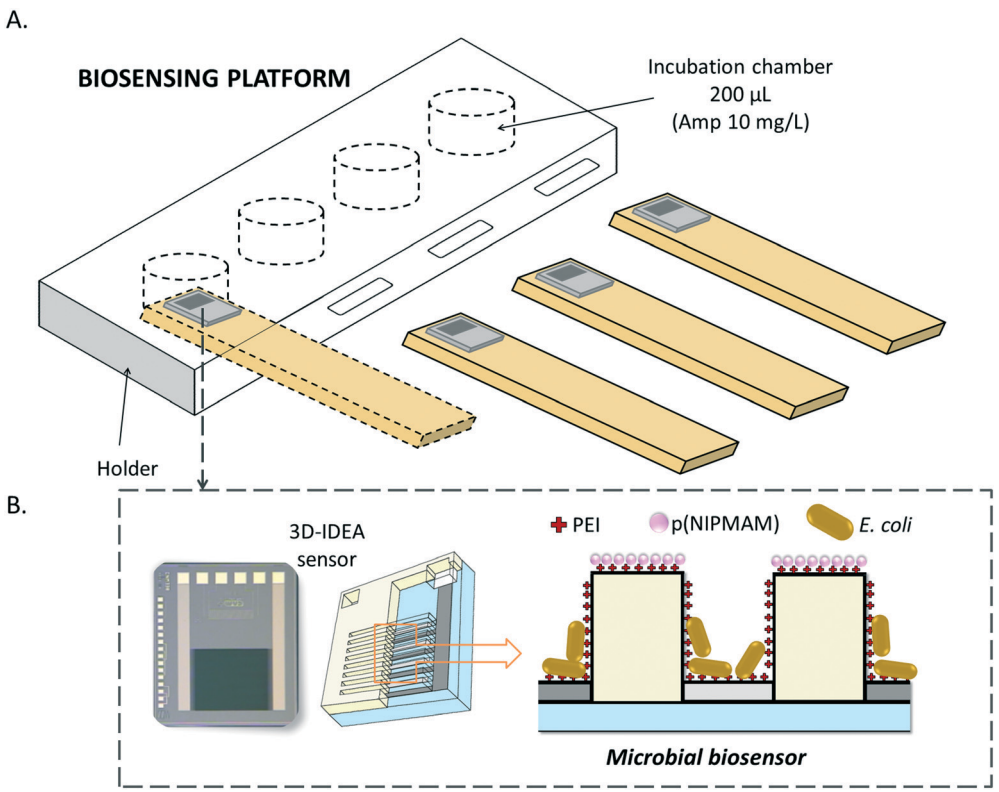


**Fig. 1** (A) Biosensing platform with the integrated (B) microbial biosensors to monitor the bacterial response to ampicillin.

 This journal is © The Royal Society of Chemistry 2019

Open Access Article. Published on 20 February 2019. Downloaded on 5/12/2025 9:43:43 PM.
This article is licensed under a Creative Commons Attribution 3.0 Unported Licence.

low pressure chemical vapor deposition (LPCVD) silicon dioxide in which electrode digits and contact pads of the transducers were opened by deep reactive ion etching (DRIE). Thus, a 4 μm high insulating barrier made of $SiO_2$ with nearly vertical walls separating the electrode digits was formed.

More detailed information and the complete technology of sensor fabrication are presented in previously published works.[22,23]

### 2.3. Synthesis and characterization of p(NIPMAM) microgels

**2.3.1. Synthesis of p(NIPMAM) microgels.** In a three-necked 250 mL flask equipped with a flat anchor-shaped mechanical stirrer, a reflux condenser and a nitrogen in- and outlet, 145 mL of water, 1.812 g (14.25 mmol, 95 mol%) of NIPMAM, 116 mg (0.75 mmol, 5 mol%) of BIS, 5 mg (0.01 mmol, 0.05%) of MRB and 69 mg (1.6 mM) of SDS were dissolved, and the reaction mixture was degassed with $N_2$ over 1 h. The solution was heated to 70 °C and the reaction was started by injecting the degassed initiator solution of 34 mg APS in 5 mL water into the reaction mixture (0.15 mmol, 1 mM). 10 min later, opalescence appeared, and the reaction was continued for a further 4 h at 70 °C and 300 rpm under a nitrogen atmosphere. The reaction mixture was cooled down to room temperature and stirred overnight. The microgel dispersion was purified by ultracentrifugation (3 times at 40 000 rpm) and followed by re-dispersion of the sediment in water. The p(NIPMAM) microgel was freeze-dried after purification for further use. The dried product was dissolved in water at 0.5 wt%.

**2.3.2. Microgel characterization**

*2.3.2.1. Zeta (ζ) potential measurements.* Electrophoretic mobility measurements were performed on a Zetasizer Nano-ZS (Malvern Instruments, Worcestershire, U.K.) in disposable capillary cells (Malvern, DTS1070) in water. Electrophoretic mobility was measured at an angle of 17° and a wavelength $\lambda$ = 633 nm of the laser beam. The ζ-potential was calculated from the electrophoretic mobility using the Smoluchowski equation.

### 2.4. Preparation of the biosensing platform

**2.4.1. 3D-IDEA modification with PEI.** First of all, 3D-IDEA sensors were cleaned with isopropanol for 10 minutes, rinsed with distilled water and dried under a nitrogen flow. To perform the deposition of PEI polycation coating on the surface, the sensors were immersed into the PEI solution for 20 minutes to form a homogeneous monolayer. Afterwards the sensors were rinsed again with distilled water and dried with a nitrogen flow.

**2.4.2. Selective p(NIPMAM) microgel immobilization on the sensor barriers by microcontact imprinting.** To attach the p(NIPMAM) microgels on top of the barriers, a two-step procedure was implemented. First, the microgels were immobilized on a flat PDMS to be used as a stamp and then transferred from the PDMS surface to the upper surface of the barriers by microcontact printing.

To immobilize the p(NIPMAM) microgels, small pieces of PDMS were initially cut with the same dimensions as 3D-IDEA chips, 3 × 3 mm. The PDMS slices were treated in an oxygen plasma system for 10 minutes at 100 mTorr and a 0.4 L $min^{-1}$ gas flow using a Diener electronic Femto plasma system (Diener Electronic GmbH, Germany) to turn the surface hydrophilic. Immediately after the microgels were sprayed 4–5 times on the treated PDMS pieces and were allowed to dry at room temperature. Afterwards, to remove the excess and to obtain a monolayer of microgels on the surface the slices were washed 3 times during 24 hours by immersing the pieces in Milli-Q water.

Once the PDMS stamp with the microgels was prepared, the microcontact printing was carried out on the 3D-IDEA sensors' surface coated with PEI to transfer the microgels on top of the barriers. To ensure the immobilization process, the microcontact printing was performed overnight or for 24 hours.

**2.4.3. Bacteria cultivation and immobilization.** Standard bacteria of the Clinical and Laboratory Standard Institute (CLSI), *Escherichia coli* ATCC 25922, were employed as model bacteria to study the response to the antibiotic ampicillin. *E. coli* was grown overnight at 37 °C in Luria-Bertani (LB) growth medium before each assay. The optical density at 600 nm (OD600) was measured and adjusted to around 0.2 ± 0.01 in LB, corresponding to a bacterial concentration of $10^8$ CFU $mL^{-1}$ (CFU – colony forming units). Bacteria cells were harvested by 10 minute centrifugation at 5000*g* and washed three times in sterile $10^{-5}$ M KCl solution. Different concentrations from $10^5$ to $10^7$ CFU $mL^{-1}$ in $10^{-5}$ M KCl were prepared by serial dilution. In the case of control experiments with ampicillin-resistant *E.coli* (*E. coli* ATCC 25922 GFP) the same growth procedure was employed. Additionally, after each test the exact bacterial concentration was determined by colony counting in LB agar plates after incubation at 37 °C for 24 hours.

To immobilize bacteria within the 3D-IDEA trenches of sensors modified with PEI coating and microgels on top of the barriers, the following procedure was applied. A drop of 10 μL of $10^{-5}$ M KCl solution containing *E. coli* cells at 5 × $10^7$ CFU $mL^{-1}$ was pipetted into the interdigitated area and maintained for 20 minutes at 37 °C. A final washing step was required to remove the cells that are not strongly bound, as well as the ones remaining on top of the barriers. The whole process is schematically represented in Fig. 2.

### 2.5. Impedance measurements

QuadTech 7600 Plus, a high precision LCR Meter analyzer, and a VeraSTAT 3F potentiostat/galvanostat (Princeton Applied Research, USA) were employed for all impedance measurements in the $10^2$–$10^6$ Hz frequency range with 100 mV (amplitude) voltage excitation. The measurements were performed in non-Faradaic mode and no DC voltage bias was

Open Access Article. Published on 20 February 2019. Downloaded on 5/12/2025 9:43:43 PM.
This article is licensed under a Creative Commons Attribution 3.0 Unported Licence.

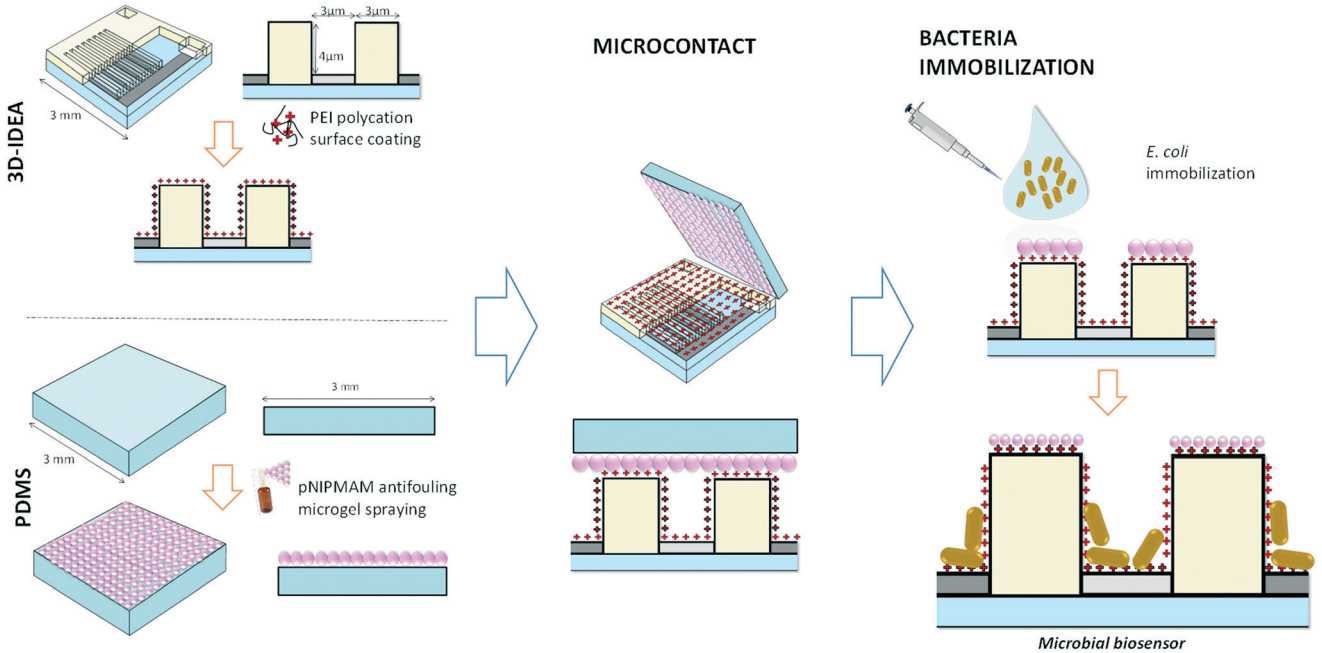


Fig. 2 Scheme of the biofunctionalization process of 3D-IDEA impedimetric transducers with *E. coli* bacteria.

applied during the impedance measurements. Impedance data treatment and equivalent circuit fitting were performed using the Z-Plot/Z-View software package (Scribner Associates, Southern Pines, NC, USA).

All experiments were done at least in triplicate using three sensors under the same conditions. Impedance measurements during the optimization and functionalization process were carried out in $10^{-5}$ M KCl solution with a controlled conductivity of 3 μS $cm^{-1}$. In the case of the microbial changes produced by antibiotics, the impedance was registered in an incubation chamber containing 200 μL of ampicillin solution at 10 μg $mL^{-1}$ with a conductivity of 3 μS $cm^{-1}$. The conductivity of the solutions employed in test experiments was controlled before and after the impedance measurements with a commercial conductimeter (EC-Meter GLP +, Crison). All the impedance measurements were carried out at controlled room temperature.

### 2.6. Microscopy imaging for characterization

Confocal laser scanning microscopy (CLSM) measurements were performed to verify the adhesion of microgels on top of the barriers and the distribution of bacteria on the 3D-IDEA surface using a LEICA TCS SP2 CLSM equipped with 40× NA 0.80 and 63× NA 0.90 water immersion objectives. To be observed using CLSM the microgels were labelled with MRB fluorescent dye and bacteria were stained using a Live/Dead Invitrogen Kit Bac Light (Invitrogen, Thermo Fisher Scientific) following the protocol detailed by the supplier.

Scanning electron microscopy (SEM) experiments were employed to accurately determine the bacterial cell distribution on the IDEA sensor. After the impedance assay, the 3D-IDEA sensors were removed from the holder and bacteria were fixed with 3% (v/v) glutaraldehyde solution in water for 16 hours and maintained at 4 °C. Then, the 3D-IDEA samples were rinsed in $H_2O$, dehydrated in graded ethanol (ranging from 50% to absolute ethanol) and air-dried using hexamethyldisilazane (HMDS), following the methodology adapted from Murtey *et al.*[36] Prior to SEM examination, samples were coated with a 20 nm gold layer with a Bio-Rad E500 sputter coater. Finally, the surface was examined using an Auriga-40 (Zeiss, Germany) SEM. PDMS stamps with microgels were dried at room temperature, coated with gold and also evaluated with SEM.

## 3. Results and discussion

### 3.1. 3D-IDEA biosensing characteristics

The sensitivity of 3D-IDEA sensors to monitor the surface changes produced by different chemical or biochemical reactions under different conditions was widely studied in previous works.[23,25,37] Electrochemical spectroscopy impedance is a powerful tool to investigate surface phenomena and changes in material bulk properties.[38] In the case of interdigitated-based sensors, the impedance in high electrolyte concentrations in the absence of a Faradaic process mainly depends on the bulk solution conductivity. However, in low conductivity solutions the surface conductivity starts to play an essential role due to the presence of surface charges.[23] In the case of 3D-IDEA sensors this effect is more pronounced because the major part of the electrical current between the electrodes goes close to the surface of the barriers and not through the surrounding bulk solution. This

 This journal is © The Royal Society of Chemistry 2019

Open Access Article. Published on 20 February 2019. Downloaded on 5/12/2025 9:43:43 PM.
This article is licensed under a Creative Commons Attribution 3.0 Unported Licence.

permits the improvement of the sensitivity of these sensors for evaluation of processes occurring on the electrode surface. Here, 3D-IDEA sensors were employed to monitor the surface functionalization steps, the bacterial immobilization, and finally, the susceptibility of bacteria to antimicrobial reagents once integrated into the biosensing platform.

The equivalent circuit employed to study the impedance response is presented in Fig. 3A and is formed by the following elements: $R_C$ is the contact resistance introduced by wires and collector bars of the thin film electrodes; $C_G$ is the geometrical (stray) capacitance between the pair of electrodes through the medium in contact (typically water solution); $R_S$ is the resistance between two electrodes of the array; $CPE_{DL}$ is a constant phase element[39] representing the capacitance of the electrical double layer at the electrode-water solution interface, attributed to the non-ideal behavior of the double layer capacitance. $R_C$ and $C_G$ are constant and depend only on the sensor geometry, while $R_S$ and $CPE_{DL}$ are variables depending on the sensor surface modification processes. As previously reported,[23] $R_S$ is a parallel combination of the bulk solution resistance ($R_{BULK}$) and the surface resistance ($R_{SURF}$), but it is important to note that under the employed experimental conditions it is not possible to distinguish these two elements in the impedance spectra. However, if the bulk solution conductivity remains fixed, we may attribute the changes in $R_S$ to alterations in the surface resistance produced by superficial reactions and modifications.[39] In consequence, the lower the bulk solution conductivity the higher the sensitivity to surface conductivity changes.[22]

The experimental impedance spectra presented in the Nyquist plot ($Z'$ *vs.* $Z''$) (Fig. 3B) allow the observation of the formation of a semicircle at high frequencies corresponding to the resistance $R_S$ in parallel with the geometrical capacitance $C_G$. The intercept with the $Z'$ axis on the left side gives the $R_C$ values, while the intercept on the right side gives the value of $R_C + R_S$, exemplified in Fig. 3B with PEI-modified electrodes, where $R_S$ is the parallel combination of $R_{BULK}$ and $R_{SURF}$. The linear response at low frequencies in the Nyquist plot is produced by a CPE of the interfacial capacitance. More details about the impedance spectra analysis are presented in the ESI.†

### 3.2. Immobilization and stability of the microgels

In order to immobilize the p(NIPMAM) antifouling microgels on top of the barriers, the 3D-IDEA surface was first modified with highly positively charged PEI acting as the anchoring layer. As observed in the Nyquist plot of Fig. 3, the absorption of PEI on the surface produced a decrease in the resistance $R_S$. Previously it was shown that adsorption of branched PEI on the sensor surface of $SiO_2$ is very fast, homogeneous and nearly irreversible.[23,40] Therefore, in this work PEI was used to immobilize the microgels on top of the barriers and *E. coli* bacteria within the trenches.

P(NIPMAM) microgels synthetized *via* precipitation polymerization employed in this study are negatively charged in aqueous solution at neutral pH according to the measured zeta potential ($\zeta = -19 \pm 3$ mV) due to the use of the negatively charged initiator APS for the polymerization. This gives the possibility of the particles to strongly adhere onto a positively charged PEI coating layer of the 3D-IDEA based on electrostatic attraction. Accordingly, the interaction of p(NIPMAM) microgels with PEI by means of microcontact printing using PDMS stamps (ESI,† Fig. S1) permitted the immobilization of microgels on top of the 3D-IDEA barriers.

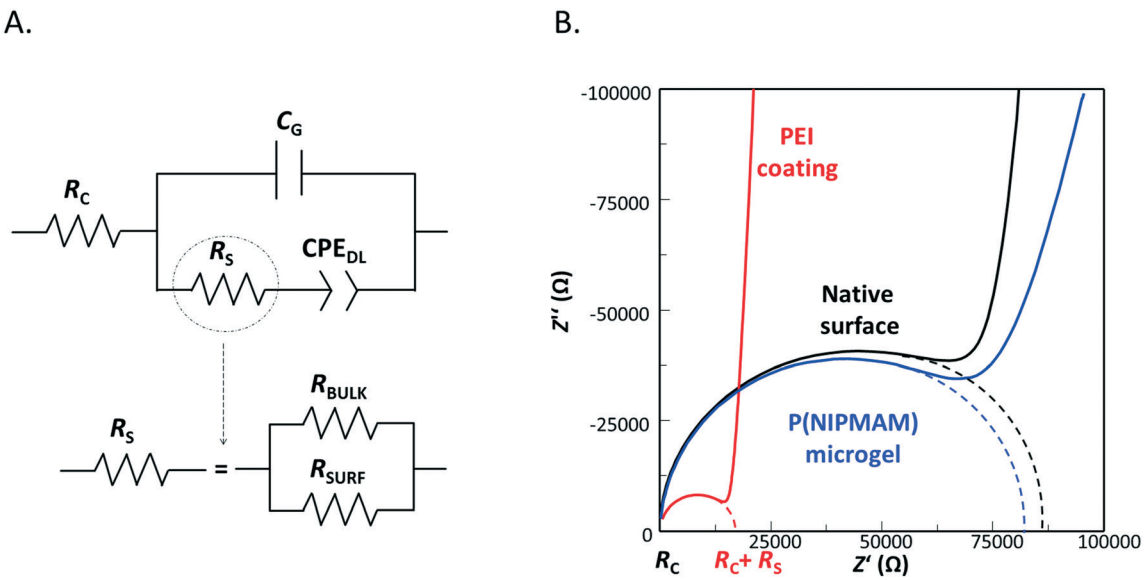


**Fig. 3** (A) Electrical equivalent circuit used for impedance spectra fitting. (B) The Nyquist plot of the 3D-IDEA measured in $10^{-5}$ M KCl solution with bare electrodes ($SiO_2$ native surface), after PEI deposition and with a p(NIPMAM) microgel on top of the barriers.

Open Access Article. Published on 20 February 2019. Downloaded on 5/12/2025 9:43:43 PM.
This article is licensed under a Creative Commons Attribution 3.0 Unported Licence.

Following from the impedance spectra observed in the Nyquist plot in Fig. 3, after p(NIPMAM) deposition by microcontact printing a significant increase in $R_S$ was observed. The changes observed in the impedance spectra demonstrate that the interaction of PEI with the p(NIPMAM) microgels is taking place. We suggest that the positive charge introduced by PEI was partially compensated by negatively charged microgels producing the increase in the surface resistance. It has to be considered that the surface modification not only provokes changes in $R_S$ but also slightly alters the interfacial capacitance (CPE) of the surface of the sensor electrodes and the electrolyte solution because of the formation of an additional layer over the barriers.

In order to confirm the correct immobilization of microgels on the surface of 3D-IDEA and, consequently, to guarantee that the microgels are localized only on top of the barriers, confocal microscopy images of the surface were obtained. Fig. 4 shows images corresponding to the surface of a 3D-IDEA sensor immersed in the $10^{-5}$ M KCl solution after the microcontact printing process. The confocal imaging was carried out in KCl solution, the same as that employed to perform the impedance measurements, in order not to alter the form of the microgels. As previously mentioned, the structure of microgels may be affected by environmental conditions, therefore, to maintain the hydrated swollen morphology p(NIPMAM) microgels were maintained in KCl solution at room temperature (25 °C)[41] (see the ESI,† Fig. S2). Thus, to reduce the variations produced by the surrounding medium all the experiments were performed in $10^{-5}$ M KCl solution.

In Fig. 4 an overlay of the imaged sections at different depths, from top to bottom of the electrodes, is presented. It can be clearly observed that microgels labelled with MRB (red color, corresponding to the emission spectra of Rhodamine B) are completely aligned along the barriers patterns, demonstrating that immobilization on top of barriers by microcontact printing was successful. Additionally, the images illustrate that at the bottom of the electrode no fluorescence was detected, confirming the spatially specific deposition of p(NIPMAM) microgels on the sensor surface. In the case of control electrodes modified only with PEI, without performing the microcontact process, no fluorescence was observed as expected (images not shown).

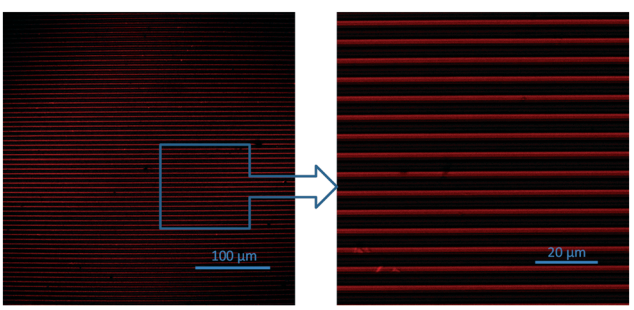


Fig. 4 Confocal microscopy image overlay of the 3D-IDEA surface after the functionalization with rhodamine-labeled (red) p(NIPMAM) microgels on top of barriers.

After the functionalization and analysis of the surface using CLSM, the stability of microgels was also evaluated by studying the impedance response of modified electrodes over time. In this case, different electrodes functionalized with PEI + p(NIPMAM) microgels and only with PEI were maintained in $10^{-5}$ M KCl solution for two days to probe the robustness of the proposed methodology and guarantee that the microgels remain on the barriers. These results are shown in Fig. 5, where changes in the determined resistance $R_S$ are monitored for two days after the corresponding functionalization of the electrodes.

Here considerable differences between two types of modifications can be observed. In the case of PEI modified electrodes the impedance of the sensors immersed in the KCl solution remained practically stable with time with only 6.03% signal variation during the first 24 hours, confirming that almost no changes on the surface occur. Sensors after the microcontact printing process presented higher initial values of $R_S$, due to the reaction between PEI and p(NIPMAM) microgels on top of the barriers. In this case a higher increase in $R_S$ was observed during the first 24 hours (12.2% variation). We suggest that during the incubation in KCl solution, the microgels reach their optimal hydration state, affecting the superficial resistance. Nevertheless, the obtained results also confirm that after this period in the KCl solution the impedance response remains completely stable in both cases.

Therefore, it was decided that before bacteria immobilization on the 3D-IDEA functionalized with PEI and microgels the sensors should remain for at least 24 hours in KCl solution to achieve stable and reproducible microgel layer properties on the surface, as well as to obtain a stable impedance response.

### 3.3. Site-specific bacterial immobilization

In order to establish the protocol of bacteria immobilization within the trenches of 3D-IDEA functionalized with p(NIPMAM) antifouling microgels on top of the barriers, different conditions were tested. First, we studied the effect of bacterial concentration and incubation time required to obtain a high density of bacteria within the trenches with high reproducibility and, at the same time, to diminish the number of bacteria on top of the barriers due to non-specific adsorption.

For this reason, a drop of 10 μL of KCl solution containing *E. coli* concentrations from $10^5$ to $10^7$ CFU mL$^{-1}$ was pipetted onto the sensor surface and incubated for either 20 or 60 minutes. At low bacteria concentrations ($10^5$ and $10^6$ CFU mL$^{-1}$) the bacteria cell density on the surface was too low and, therefore, these concentrations were omitted considering that a reduced quantity of bacteria in the trenches would not produce a significant response to ampicillin.

 This journal is © The Royal Society of Chemistry 2019

Open Access Article. Published on 20 February 2019. Downloaded on 5/12/2025 9:43:43 PM.
This article is licensed under a Creative Commons Attribution 3.0 Unported Licence.

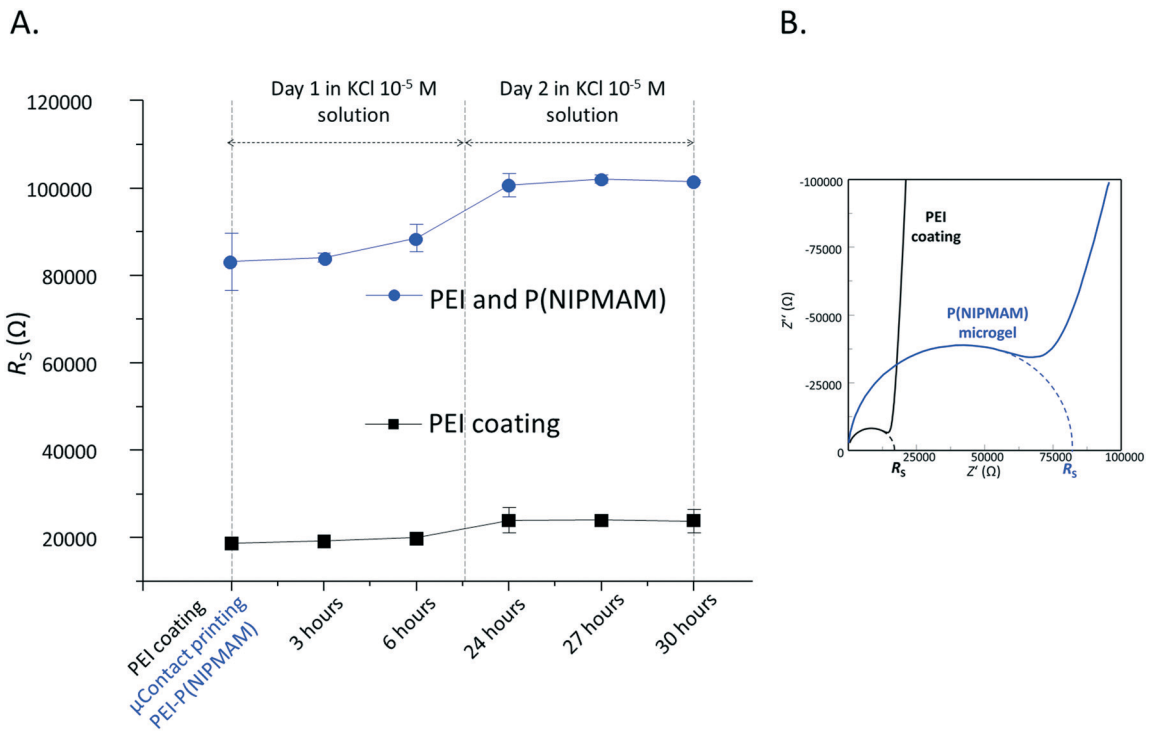


**Fig. 5** (A) $R_S$ resistance variations in $10^{-5}$ M KCl solution for 3D-IDEA sensors modified with PEI (black squares) and PEI-p(NIPMAM) microgels (blue circles) with time and (B) the Nyquist plot corresponding to the impedance spectra after each modification.

CLMS images of the electrode surfaces were acquired to compare the bacteria distribution of *E. coli* immobilized on the 3D-IDEA surface using a concentration of $10^7$ CFU $mL^{-1}$ depending on the incubation time. Live/Dead images corresponding to bacteria distribution after 20 and 60 minutes of incubation are presented in Fig. S3a and S3b of the ESI.† It was observed that after 20 minutes the majority of bacteria were located at the bottom of the electrodes (in trenches) as desired, and just a few bacteria remained on top of the barriers. In contrast, after 60 minutes of incubation a large amount of microorganisms was observed on top of the barriers as well as in the trenches. Here, it is worth noting that after 60 minutes the drop of 10 µL of KCl solution containing *E. coli* bacteria was completely evaporated and may facilitate the fixation of bacteria on top of the barriers even in the presence of antifouling microgels. Based on these data 20 minutes was chosen as the optimal time for bacteria immobilization.

In addition, to observe the distribution of bacteria with and without microgels on top of the barriers SEM images of the surface were also acquired after 20 minutes of incubation. Thus, the distributions of bacteria on the electrodes modified with PEI + p(NIPMAM) microgels and only with PEI were compared, as shown in Fig. 6.

Here it can be clearly seen that the electrodes modified with PEI and the p(NIPMAM) microgels on top of the barriers present the majority of bacteria within the trenches (-Fig. 6A, C and E). In the case of electrodes modified with PEI, bacteria are homogeneously distributed on the entire surface, both in the trenches and on top of the barriers (-Fig. 6B, D and F). These results are also in accordance with those obtained by confocal imaging (see Fig. S3a. A and B†). This proves the effectiveness of the p(NIPMAM) microgels as an antifouling agent to prevent bacterial attachment, which was also demonstrated recently in more detail.[34]

Accordingly, the reproducibility of bacteria immobilization on a sensor surface may be evaluated in terms of the impedance response after *E. coli* immobilization with 3D-IDEA modified with PEI and the p(NIPMAM) microgels and only with PEI. In the first case, $R_S$ absolute values present a reproducibility of 92.5% ($n$ = 9) with bacteria within the trenches, while only 71% ($n$ = 6) was observed when bacteria are distributed on the entire surface modified with PEI. Here, it is important to note that the methodology employed for the deposition of bacteria guarantees their significant concentration within the trenches with high reproducibility. Therefore, under the experimental conditions employed bacteria are maintained only in KCl solution without essential nutrients. This should prevent the division of bacteria cells and it can be assumed that bacteria are not growing, and their concentration on the sensor surface is constant, thus reducing the subsequent variability problems that they could produce in the impedance response.

In summary, the obtained results give the evidence that the optimal conditions for selective immobilization of *E. coli* within the 3D-IDEA trenches are 20 minutes of incubation using $10^7$ CFU $mL^{-1}$ bacteria solution. Under these conditions it was possible to establish a reproducible and

Open Access Article. Published on 20 February 2019. Downloaded on 5/12/2025 9:43:43 PM.
This article is licensed under a Creative Commons Attribution 3.0 Unported Licence.

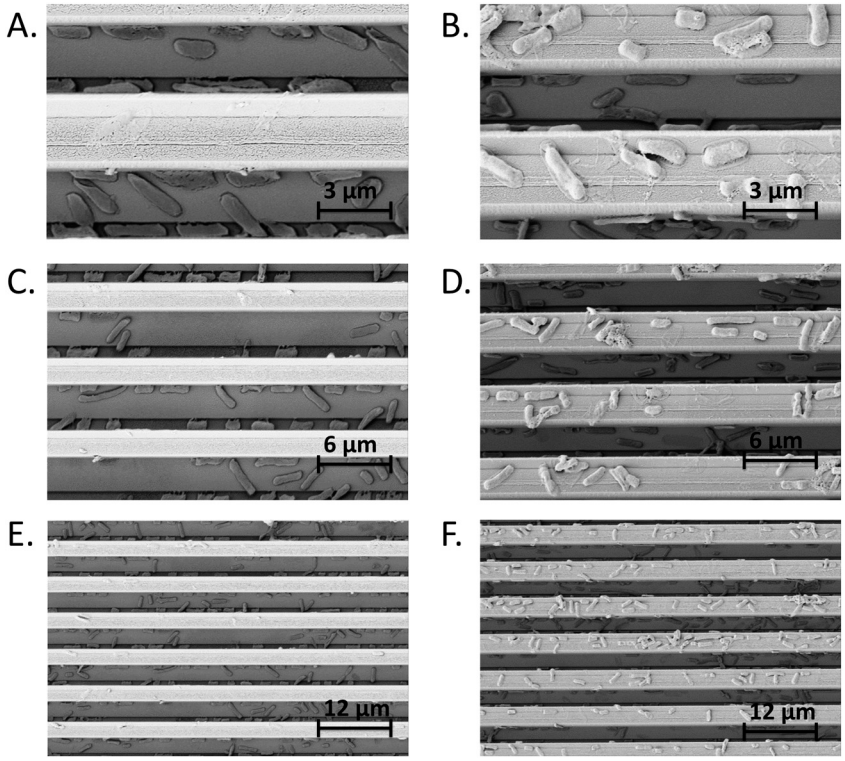


**Fig. 6** SEM images corresponding to the 3D-IDEA surface after deposition of *E. coli* bacteria for 20 minutes with PEI and p(NIPMAM) modified electrodes (A, C and E) and only with PEI (B, D and F) at different magnifications (×5000 (A and B), ×10 000 (C and D) and ×20 000 (E and F)).

controlled methodology to perform bacterial immobilization on cell-based biosensors, which is a crucial point in their application for different sample testing.[42]

### 3.4. Integration of biosensors into the biosensing platform and monitoring of bacterial response to ampicillin

To validate the proposed microbial biosensor approach and demonstrate its effectiveness, experiments were conducted with sensors integrated into the biosensing platform, which consists of a specifically designed holder (Fig. 1) with a 200 μL chamber over each individual sensor. Four 3D-IDEA sensors were introduced into the holder chamber to perform impedance measurements in 200 μL of solutions with controlled low conductivity (Fig. 1). The chambers were sealed hermetically to prevent solution evaporation. The use of solutions with reduced volumes at low conductivity allows easy monitoring of the changes produced in $R_S$ as a result of metabolic processes or the release of ionic products by bacteria.[43] This integrated biosensing system was used to study the developed *E. coli* bacterial biosensor impedance response to ampicillin as an antimicrobial agent.

*E. coli* ATCC 25922 is a reference strain with well-established minimum inhibitory (MIC) and minimal bactericidal concentration (MBC) values obtained by different antimicrobial susceptibility assays. MIC and MBC correspond to the lowest concentration of an antimicrobial reagent that prevents or kill bacteria, respectively.[8,9] The MIC values for ampicillin are about 2–8 mg $L^{-1}$ and MBC mean values are around 8.8 mg $L^{-1}$.[44,45] The objective of this work is to study the effect of ampicillin on the cell integrity of *E. coli* immobilized on the sensor surface by means of registering the impedance alterations. An ampicillin concentration of 10 mg $L^{-1}$ was selected, which is slightly higher than the MBC values, to guarantee that ampicillin has a bactericidal effect. Additionally, the bactericidal effect of this ampicillin concentration was probed using standard protocols (ESI,† Fig. S5).

In order to evaluate the effectiveness of the proposed approach sensors modified in different ways were compared. 3D-IDEA sensors functionalized with microgels on top of the barriers and *E. coli* within the trenches were incubated in a solution of $10^{-5}$ M KCl supplemented with ampicillin at 10 mg $L^{-1}$ and the variations in the impedance were monitored for 24 hours in the designed low volume biosensing system. It has to be noted that ampicillin at this concentration practically does not affect the conductivity of KCl solution, which is a relevant aspect to consider in the impedance measurements under these conditions.

Control measurements were performed using electrodes functionalized under different conditions. First, the same sensors with the microgels and *E. coli* but without ampicillin were used to test if the impedance response remained stable. Another control using 3D-IDEA with the microgels and without *E. coli* was also monitored in the presence of ampicillin. Finally, to demonstrate the higher sensitivity of our approach, in which the p(NIPMAM) antifouling microgels on

 This journal is © The Royal Society of Chemistry 2019

Open Access Article. Published on 20 February 2019. Downloaded on 5/12/2025 9:43:43 PM.
This article is licensed under a Creative Commons Attribution 3.0 Unported Licence.

top of the barriers allow the improvement of the immobilization of bacteria in the trenches, the same conditions were employed but using 3D-IDEA functionalized exclusively with PEI and *E. coli*. In this case, as demonstrated in Fig. 6, bacteria cells are distributed homogeneously on the sensor surface, within the trenches as well as on top of the barriers. The corresponding results are presented in Fig. 7.

The impedance response, $\Delta R_S$, presented as the variation of $R_S$ during the reaction process, was calculated as follows:

$$\Delta R_S = R_S^{Amp} - R_S^0, \quad (1)$$

where $R_S^0$ corresponds to the resistance of sensors before applying ampicillin, and $R_S^{Amp}$ corresponds to resistance after addition of ampicillin.

3D-IDEA sensors with microgels and *E. coli* cells in the trenches in the presence of ampicillin experienced a large decrease in $R_S$ mainly in the first 1–2 hours, and the signal remained quite stable from the fourth hour onwards. Under these conditions, we assume that ampicillin was affecting the cell membrane of bacteria producing its progressive disruption and the release of the cytoplasmic content into the surrounding solution. The cytoplasm of bacteria is formed by different dissolved charged macromolecules and ions,[46] thus during bacterial lysis these components are washed out into the surrounding KCl solution increasing its conductivity and, consequently, decreasing the solution resistance. Moreover, as bacteria are located within the 3 μm wide trenches the diffusion of electrolyte from the trench to the outer solution is impeded and this possibly enhances the response.

At the same time, no significant changes in the impedance response were observed in control experiments. The functionalized sensors in KCl solution without ampicillin were stable over time, confirming that *E. coli* bacteria on the surface remained intact. The 3D-IDEA control with microgels on top of the barriers without bacteria also remained invariable, demonstrating that ampicillin does not interact with the sensor. In all the cases the response was stable during 5–6 hours of the measurements.

In principle, in the presence of 10 μM KCl the low osmotic pressure may stress the bacterial cells affecting their viability. However, in Fig. 7A and B (blue line) it can be observed that the microbial biosensor in the low conductivity solution (KCl $10^{-5}$ M) shows a really stable response over time. Therefore, it demonstrates that the integrity of bacterial cells is maintained because no changes in the impedance response are observed. This fact validates that within the performed methodology bacterial cells remain alive in the KCl solution employed. In contrast, when the assays are performed with ampicillin, a significant change in impedance is observed, indicating the lysis of *E. coli* cells.

In addition, Fig. 7A shows that sensors without microgels and only coated with PEI with immobilized *E. coli* cells also presented a decrease in the $R_S$ values. This demonstrates that ampicillin is affecting the integrity of bacteria in a similar way as explained above. However, the sensitivity of this type of sensor is considerably lower. This ratifies the importance of concentrating bacteria within the trenches of 3D-IDEA impedance-based sensors in order to obtain better reproducibility and higher sensitivity, and it accentuates the role of

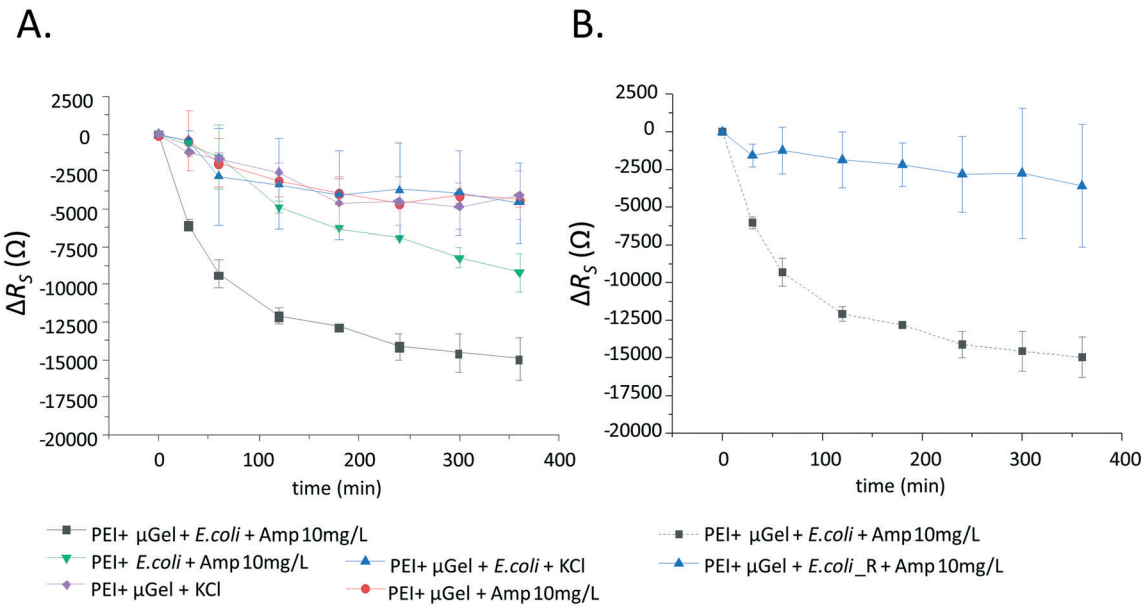


**Fig. 7** A) $R_S$ variations with time of 3D-IDEA sensors modified with PEI-p(NIPMAM) μGel and *E. coli* in KCl solution with Amp at 10 mg $L^{-1}$ (black), PEI-p(NIPMAM) μGel with Amp at 10 mg $L^{-1}$ (red), PEI-p(NIPMAM) μGel in KCl solution (violet), PEI-p(NIPMAM) μGel and *E. coli* in KCl solution (blue), and PEI modified electrodes with *E. coli* in KCl solution with Amp at 10 mg $L^{-1}$ (green). B) $R_S$ variations with time measured in KCl solution with Amp at 10 mg $L^{-1}$ of 3D-IDEA sensors modified with PEI-p(NIPMAM) μGel and *E. coli* ATCC 25922 (non-resistant to Amp) in black compared with *E. coli* ATCC 25922GLP (resistant to Amp) in blue.

Open Access Article. Published on 20 February 2019. Downloaded on 5/12/2025 9:43:43 PM.
This article is licensed under a Creative Commons Attribution 3.0 Unported Licence.

antifouling microgels on top of the barriers to achieve this. The proposed approach allows detecting the microbial susceptibility to ampicillin in a short detection time (1 or 2 hours) as compared to other tests based on culturing methods that require between 18 and 48 h to provide results.[8,47] In addition, to corroborate the bactericidal effect of ampicillin on the bacteria, Live/Dead images of the sensor surface with bacteria were obtained after the impedance measurements, confirming that *E. coli* cells were dead (see Fig. S4 of the ESI†).

In parallel, to validate that the changes in impedance were caused by the cell damage provoked by ampicillin, an identical study with an ampicillin-resistant *E. coli* strain was carried out. The susceptibility of the two strains to ampicillin was previously tested showing sensitivity in *E. coli* ATCC 25922 and resistance in *E. coli* ATCC 25922GLP for the tested antibiotic (see the ESI,† Fig. S5).

Fig. 7B shows the impedimetric response of the ampicillin resistant and non-resistant *E. coli* in the presence of ampicillin. In the case of resistant *E. coli* there were no changes in $R_S$ indicating that ampicillin does not affect the viability of bacteria as expected.

According to these results, the proposed novel method to functionalize the barrier surface of 3D-IDEA sensors with p(NIPMAM) microgels, the strategy to selectively immobilize bacteria within the trenches and the subsequent monitoring of impedance changes related to the bactericidal effect of ampicillin to *E. coli* cells have been demonstrated. The developed approach is a versatile, rapid, compact and easy-to-use platform based on the microbial biosensor concept that can be useful in a wide spectrum of toxicity monitoring-related applications.

## 4. Conclusions

This work presents a microbial biosensor approach focused on the development of a novel and reproducible strategy based on the immobilization of *E. coli* bacteria on a three-dimensional interdigitated electrode array (3D-IDEA) impedimetric transducer. The developed microbial sensor was employed in a biosensing platform especially designed to monitor the bacterial response to the antibiotic ampicillin. Surface functionalization, bacteria immobilization and the microbial response to ampicillin were characterized with the EIS technique that allows registering variations in superficial resistance provoked in each modification step.

To improve the reproducibility of the immobilization and the sensitivity to the bacterial response, *E. coli* cells were selectively immobilized within the 3D-IDEA trenches between the insulating barriers. One of the main novelties is the modification of the top of the barriers with antifouling poly(*N*-isopropylmethacrylamide) (p(NIPMAM)) microgels in order to prevent the deposition of bacteria. To achieve selective deposition, the microgels were first immobilized on a PDMS substrate and afterwards transferred to the sensor surface *via* a microcontact printing procedure. The polycation polyethyleneimine (PEI) was employed as the assembling layer of *E. coli* cells in the trenches as well for the p(NIPMAM) microgels on the barriers. The suitability of the proposed immobilization method was demonstrated by confocal microscopy and scanning electron microscopy imaging confirming that *E. coli* bacteria are located within the trenches. In addition, for 3D-IDEA sensors with the microgels on top of the barriers the reproducibility in terms of $R_S$ values after *E. coli* immobilization is about 92.5% and only 71% when bacteria are distributed on the entire surface modified only with PEI.

The applicability of the developed microbial biosensor was studied by introducing the functionalized devices into the designed small volume biosensing system containing a bactericidal concentration of ampicillin (10 mg $L^{-1}$) in $10^{-5}$ M KCl solution. The impedance changes in terms of $R_S$ show a decrease attributed to the release of cytoplasmic components, promoted by the lysis of bacterial cell membrane, and demonstrating the response and sensibility to ampicillin. Accordingly, the same procedure was employed with an *E. coli* strain resistant to ampicillin, and no significant impedance changes were observed.

To sum up, the developed microbial biosensing approach may be very interesting in a broad spectrum of applications related to toxicity evaluation. In addition, the same procedure can be applied to study any other types of bacteria and their susceptibility to different antibacterial reagents.

## Author contribution

S. B. O and O. M. carried out the experiment and data analysis. N. U and N. A. provided expertize on experiments planning. S. B. O. wrote the original draft manuscript. S. B. O., N. A., N. U., A. B. and P. v. R. conceived the original idea. N. A., P. v. R and A. B. supervised the findings of this work. O. M., A. B. and P. v. R. were in charge of overall direction and planning. All authors provided critical feedback and helped shape the research, analysis and manuscript.

## Conflicts of interest

There are no conflicts of interest to declare.

## Acknowledgements

The authors acknowledge financial support from the Spanish Ministry of Economy and Competitiveness (project CTQ2014-54553-C3-1-R, CTQ2015-66254-C2-2-P and S. B. O fellowship BES-2015-071250). S. B. O. also acknowledges the PhD program in Biotechnology of Universitat Autònoma de Barcelona. O. M. is grateful for financial support from the Alexander von Humboldt Foundation.

## References

1 M. Vouga and G. Greub, *Clin. Microbiol. Infect.*, 2016, **22**, 12–21.

 This journal is © The Royal Society of Chemistry 2019

Open Access Article. Published on 20 February 2019. Downloaded on 5/12/2025 9:43:43 PM.
This article is licensed under a Creative Commons Attribution 3.0 Unported Licence.

2 J. Davies and D. Davies, *Microbiol. Mol. Biol. Rev.*, 2010, **74**, 417–433.
3 K. Kümmerer, *Chemosphere*, 2009, **75**, 417–434.
4 V. K. Sharma, *Chemosphere*, 2016, **150**, 702–714.
5 J. Bengtsson-Palme, *FEMS Microbiol. Rev.*, 2018, **42**, 68–80.
6 C. Cháfer-Pericás, Á. Maquieira and R. Puchades, *TrAC, Trends Anal. Chem.*, 2010, **29**, 1038–1049.
7 A. van Belkum, T. T. Bachmann, G. Lüdke, J. G. Lisby, G. Kahlmeter, A. Mohess, K. Becker, J. P. Hays, N. Woodford, K. Mitsakakis, J. Moran-Gilad, J. Vila, H. Peter, J. H. Rex, W. M. Dunne Jr and The JPIAMR AMR-RDT Working Group on Antimicrobial Resistance and Rapid Diagnostic Testing, *Nat. Rev. Microbiol.*, 2019, **17**, 51–62.
8 L. B. Reller, M. Weinstein, J. H. Jorgensen and M. J. Ferraro, *Clin. Infect. Dis.*, 2009, **49**, 1749–1755.
9 M. Balouiri, M. Sadiki and S. K. Ibnsouda, *J. Pharm. Anal.*, 2016, **6**, 71–79.
10 Ö. Baltekin, A. Boucharin, E. Tano, D. I. Andersson and J. Elf, *Proc. Natl. Acad. Sci. U. S. A.*, 2017, **114**, 9170–9175.
11 P. Athamanolap, K. Hsieh, L. Chen, S. Yang and T.-H. Wang, *Anal. Chem.*, 2017, **89**, 11529–11536.
12 V. Gaudin, *Biosens. Bioelectron.*, 2017, **90**, 363–377.
13 A. M. Ferrini, V. Mannoni, G. Carpico and G. E. Pellegrini, *J. Agric. Food Chem.*, 2008, **56**, 784–788.
14 M. Espinosa-Urgel, L. Serrano, J. L. Ramos and A. M. Fernández-Escamilla, *Mol. Biotechnol.*, 2015, **57**, 558–564.
15 F.-D. Munteanu, A. M. Titoiu, J.-L. Marty and A. Vasilescu, *Sensors*, 2018, **18**, 901.
16 A. Bratov, S. Brosel-Oliu and N. Abramova, in *Label-Free Biosensing: Advanced Materials, Devices and Applications*, ed. M. J. Schöning and A. Poghossian, Springer International Publishing, Cham, 2018, pp. 179–198.
17 L. Yang and R. Bashir, *Biotechnol. Adv.*, 2008, **26**, 135–150.
18 C. Berggren, B. Bjarnason and G. Johansson, Capacitive Biosensors, *Electroanalysis*, 2001, **13**, 173–180.
19 J. S. Daniels and N. Pourmand, *Electroanalysis*, 2007, **19**, 1239–1257.
20 A. Guimerà, G. Gabriel, E. Prats-Alfonso, N. Abramova, A. Bratov and R. Villa, *Sens. Actuators, B*, 2015, **207**, 1010–1018.
21 M. Varshney and Y. Li, *Biosens. Bioelectron.*, 2009, **24**, 2951–2960.
22 S. Brosel-Oliu, D. Galyamin, N. Abramova, F.-X. Muñoz-Pascual and A. Bratov, *Electrochim. Acta*, 2017, **243**, 142–151.
23 A. Bratov and N. Abramova, *J. Colloid Interface Sci.*, 2013, **403**, 151–156.
24 S. Brosel-Oliu, R. Ferreira, N. Uria, N. Abramova, R. Gargallo and F.-X. Muñoz-Pascual, *et al.*, *Sens. Actuators, B*, 2018, **255**, 2988–2995.
25 M. Hoyos-Nogués, S. Brosel-Oliu, N. Abramova, F.-X. Muñoz, A. Bratov and C. Mas-Moruno, *et al.*, *Biosens. Bioelectron.*, 2016, **86**, 377–385.
26 R. M. Epand, C. Walker, R. F. Epand and N. A. Magarvey, *Biochim. Biophys. Acta, Biomembr.*, 2016, **1858**, 980–987.
27 M. A. Kohanski, D. J. Dwyer and J. J. Collins, *Nat. Rev. Microbiol.*, 2010, **8**, 423–435.
28 D. J. McClements, *Adv. Colloid Interface Sci.*, 2017, **240**, 31–59.
29 J. Tavakoli and Y. Tang, *Polymer*, 2017, **9**, 364.
30 D. Buenger, F. Topuz and J. Groll, *Prog. Polym. Sci.*, 2012, **37**, 1678–1719.
31 N. M. B. Smeets and T. Hoare, *J. Polym. Sci., Part A: Polym. Chem.*, 2013, **51**, 3027–3043.
32 A. B. South, R. E. Whitmire, A. J. García and L. A. Lyon, *ACS Appl. Mater. Interfaces*, 2009, **1**, 2747–2754.
33 S. Schmidt, M. Zeiser, T. Hellweg, C. Duschl, A. Fery and H. Möhwald, *Adv. Funct. Mater.*, 2010, **20**, 3235–3243.
34 D. Keskin, O. Mergel, H.-C. van der Mei, H.-J. Busscher and P. van Rijn, *Biomacromolecules*, 2019, **20**, 243–253.
35 Y. Lvov, K. Ariga, I. Ichinose and T. Kunitake, *Thin Solid Films*, 1996, **284-285**, 797–801.
36 M. D. Murtey and P. Ramasamy, in *Modern Electron Microscopy in Physical and Life Sciences*, ed. M. Janecek, InTech, 2016, pp. 161–185.
37 A. Bratov, N. Abramova, M. P. Marco and F. Sanchez-Baeza, *Electroanalysis*, 2012, **24**, 69–75.
38 Y. Li, R. Afrasiabi, F. Fathi, N. Wang, C. Xiang and R. Love, *et al.*, *Biosens. Bioelectron.*, 2014, **58**, 193–199.
39 A. Bratov, N. Abramova, J. Ramón-Azcón, A. Merlos, F. Sánchez-Baeza and M.-P. Marco, *et al.*, *Electrochem. Commun.*, 2008, **10**, 1621–1624.
40 M. Kolasińska, R. Krastev and P. Warszyński, *J. Colloid Interface Sci.*, 2007, **305**, 46–56.
41 L. V. Sigolaeva, S. Y. Gladyr, A. P. H. Gelissen, O. Mergel, D. V. Pergushov and I. N. Kurochkin, *et al.*, *Biomacromolecules*, 2014, **15**, 3735–3745.
42 Q. Gui, T. Lawson, S. Shan, L. Yan and Y. Liu, *Sensors*, 2017, **17**, 1623.
43 N. Uria, J. Moral-Vico, N. Abramova, A. Bratov and F. X. Muñoz, *Electrochim. Acta*, 2016, **198**, 249–258.
44 A. Hakanen, P. Huovinen, P. Kotilainen, A. Siitonen and H. Jousimies-Somer, *J. Clin. Microbiol.*, 2002, **40**, 2705–2706.
45 L. G. Reimer, C. W. Stratton and L. B. Reller, *Antimicrob. Agents Chemother.*, 1981, **19**, 1050–1055.
46 J. T. Trevors, *Int. J. Mol. Sci.*, 2011, **12**, 1650–1659.
47 F. Pujol-Vila, J. Dietvorst, L. Gall-Mas, M. Díaz-González, N. Vigués and J. Mas, *et al.*, *J. Colloid Interface Sci.*, 2018, **511**, 251–258.